J Ind Microbiol Biotechnol (2012) 39:1507–1514
DOI 10.1007/s10295-012-1147-4

Temporal analysis of xylose fermentation by *Scheffersomyces stipitis* using shotgun proteomics

Eric L. Huang · Mark G. Lefsrud

Received: 13 February 2012 / Accepted: 3 May 2012 / Published online: 26 May 2012

Abstract Proteomics and fermentation technology have begun to integrate to investigate fermentation organisms in bioprocess development. This is the first shotgun proteomics study employed to monitor the proteomes of *Scheffersomyces stipitis* during xylose fermentation under oxygen limitation. We identified 958 nonredundant proteins and observed highly similar proteomes from exponential to early stationary phases. In analyzing the temporal proteome, we identified unique expression patterns in biological processes and metabolic pathways, including alternative respiration salicylhydroxamic acid (SHAM) pathway, activation of glyoxylate cycle, expression of galactose enzymes, and secondary zinc-containing alcohol dehydrogenase and *O*-glycosyl hydrolases. We identified the expression of a putative, high-affinity xylose sugar transporter Xut1p, but low-affinity xylose transporters were absent. Throughout cell growth, housekeeping processes included oxidative phosphorylation, glycolysis, nonoxidative branch of the pentose phosphate pathway, gluconeogenesis, biosynthesis of amino acids and aminoacyl total RNA (tRNA), protein synthesis and proteolysis, fatty acid metabolism, and cell division. This study emphasized qualitative analysis and demonstrated that shotgun proteomics is capable of monitoring *S. stipitis* fermentation and identifying physiological states, such as nutrient deficiency.

Keywords Shotgun proteomics · MudPIT · *Scheffersomyces stipitis* · *Pichia stipitis* · Fermentation monitoring

Introduction

Scheffersomyces stipitis (synonymy *Pichia stipitis*) has gained research interests due to near theoretical ethanol yield and low xylitol yield from pentose. The expressions of various novel hemicellulolytic α-glucuronidases and xylosidases give further industrial promises in lignocellulose bioconversion [35]. With the biochemistry and physiology of xylose fermentation characterized, researchers have conducted extensive research to investigate *S. stipitis* ethanol fermentation with the ultimate goal of economical ethanol production using lignocellulosic hydrolysate. The complete sequenced and assembled genome of *S. stipitis* (*P. stipitis* CBS 6054) provides the insight into this peculiar yeast and enables researchers to perform large-scale analysis of *S. stipitis* transcriptomics and proteomics [16]. A more systematic approach to studying *S. stipitis* fermentation is needed, and system biology and fermentation technology can be more fully integrated with advanced high-throughput proteomic techniques, such as multidimensional protein identification technology (MudPIT) [21, 44, 47]. MudPIT allows observation of the global profile of the organism's proteome, such as yeast, and analysis of the proteome allows evaluation of yeast physiology at greater depth with a much simpler technique than 2D polyacrylamide gel electrophoresis mass spectrometry (PAGE-MS) [44]. In fermentation technology, researchers have applied metabolomics in bioprocessing to find targets for metabolic engineering and biomarkers for clone selection or media development [27]. In proteomics, *S. cerevisiae* proteome

Electronic supplementary material The online version of this article (doi:10.1007/s10295-012-1147-4) contains supplementary material, which is available to authorized users.

E. L. Huang · M. G. Lefsrud (✉)
Bioresource Engineering, McGill University,
21111 Lakeshore Road, Ste-Anne-de-Bellevue,
QC H9X 3V9, Canada
e-mail: mark.lefsrud@mcgill.ca

under stress conditions in lignocellulosic hydrolysate was studied and exhibited differential expression in tricarboxylic acid cycle (TCA) cycle and glycolysis, potentially a guideline for process development in future lignocellulosic ethanol production [20]. Also, shotgun proteomic profiling of *Clostridium acetobutylicum* from the butanol fermentation process was carried out to elucidate the molecular functional mechanisms in butanol production [39]. Monitoring the proteome of *S. stipitis* throughout the growth cycle could be used to investigate and elucidate cell stress, stages in cell cycles, nutrient deficiency, cell death, and even to discover metabolic pathways.

The analysis of genome and expression-array studies provided insights into central carbon metabolism and specialized physiological traits in *S. stipitis* [17]. However, the study reported here is the first shotgun proteomics study of xylose fermentation by *S. stipitis* on the proteome level. The study focused on qualitative analysis of the proteome and in some cases provided semiquantitative data of relative abundance based on spectral counts. Shotgun proteomics supported the predicted protein coding regions in the *S. stipitis* genome, and in analyzing the temporal proteome of *S. stipitis,* we discovered proteins expressed in peculiar metabolic pathways and that exhibited unique expression patterns when compared with the well-studied model organism *S. cerevisiae*, even though the structures of many core-function gene-coding regions are highly similar between the two [17]. Shotgun proteomics also showed the physiological state of *S. stipitis* during fermentation.

Materials and methods

Microorganism and culture conditions

*Scheffersomyces stipitis (*a.k.a. *P. stipitis* CBS 6054) was obtained from American Type Culture Collection (Manassas, VA, USA) and maintained on YPX agar slants (20 g/L xylose, 20 g/L peptone, 20 g/L Difco Bacto-Agar and 10 g/L yeast extract) (BD-Canada, Mississauga, ON, Canada). Inoculums were grown in YPX at 26 °C for ~20 h at 100 rpm until the optical density at 600 nm (OD_{600}) reached ~2. Xylose fermentation of *S. stipitis* was carried out using a 250 -ml Erlenmeyer flask with 100-ml working volume at 26 °C in the incubator at 100 rpm. Medium composition for *S. stipitis* xylose fermentation was 20 g/L xylose, 20 g/L peptone, and 10 g/L yeast extract.

Fermentation parameters analysis

Xylitol concentration was measured using the R-Biopharm enzymatic assay kit (Darmstadr, Germany). Xylose, ethanol, and glycerol were measured using Megazyme enzymatic assay kits (Wicklow, Ireland). *S. stipitis* growth was monitored by measuring the OD_{600} with an ultraviolet visual spectroscopy (UV–VIS) spectrophotometer.

Cells lysis and protein extraction

Three protein samples were taken throughout the growth cycle at 25, 45.5, and 64 h. Approximately10 mg of dry-mass cell pellet for each sample was obtained and processed through single-tube cell lysis and protein digestion [40, 42]. Protein concentrations were ~6 mg/ml for each sample after extraction. Tris/10 mM calcium chloride ($CaCl_2$) at pH 7.6 and 6 M guanidine/10 mM dithiothreitol (DTT) (Sigma-Aldrich Canada, Oakville, ON, Canada) were used to lyse cells and extrude proteins. In brief, the mixture was placed on the rocker for the first hour and vortexed every 10 min and then incubated for 12 h at 37 °C. The mixture was spun down at 10,000 g. The supernatant was discarded and the pellet was diluted with sixfold 50 mM Tris/10 mM $CaCl_2$. Approximately 5 μg of sequencing-grade trypsin (Promega, Madison, WI, USA) was added to each sample and digested for 12 h at 37 °C by gentle rocking. The same amount of trypsin was added a second time and incubated at 37 °C for another 12 h; 1 M DTT was added to a final concentration of 20 mM and incubated for another hour with gentle rocking at 37 °C, followed by centrifugation at 10,000*g* for 10 min. The supernatant was kept and samples were cleaned and desalted via solid-phase extraction with Sep-Pak Plus cartridges (Waters Limited, Mississauga, ON, Canada), concentrated, solvent exchanged, filtered, aliquotted, and frozen at −80 °C [46].

2D-LC MS/MS

Each extracted and digested sample was analyzed twice to achieve technical replications in 2D liquid chromatography tandem mass spectroscopy (LC MS/MS). Samples were loaded onto the back column of a split-phase 2D column [26] (~3–5 cm Luna SCX 5 μm and ~3–5 cm C_{18} Aqua 5 μm 100A) (Phenomenex, Torrance, CA, USA) using a pressure cell and then connected to a front column with an integrated nanospray tip (~15 cm of Aqua C_{18} Aqua 5 μm 100A, Phenomenex; 150 μm with 15 μm tip, New Objective, Woburn, MA, USA). Samples were analyzed via 2D LC-nano electrospray ionization (ESI)-MS/MS on a Thermo LTQ (ThermoFisher Scientific, San Jose, CA, USA), as previously described [31, 42]. Samples were analyzed via 13-h (6 step with 1 wash step) runs [26, 46].

Proteome informatics

Proteome Discoverer 1.1 (ThermoFisher Scientific) and the SEQUEST algorithm [8] were used to correlate peptide

spectra with the *S. stipitis* protein-sequence filtered models containing 5,839 entries downloaded from the Joint Genome Institute (http://genome.jgi.doe.gov/Picst3/Picst3.home.html; downloaded on 05/15/2011) [16]. Proteome Discoverer 1.1 was used to filter SEQUEST results and sort peptides into protein identification based on a modified method of Verberkmoes et al. [42] (minimum Xcor of at least 1.5 [+1], 2.3 [+2], 2.8 [+3]; minimum probability score of at least 2 [+1], 7 [+2] and 7.5 [+3]; minimum two fully tryptic peptides and at least one unique peptide among the two fully tryptic peptides). We enabled protein grouping, counted only rank 1 peptides, and only in the top-scored proteins. Reverse protein sequences of *S. stipitis* were included in the search database to estimate the overall false-positive rates of protein identification using the reverse database method (false positive rate $= 2[n_{rev}/(n_{rev} + n_{real})] * 100$; n_{rev} = number of peptides identified from the reverse database; n_{real} = number of peptides identified from the real database) [30]. Differentially expressed proteins between time points were calculated based on the spectral counts using the software PatternLab [4]. AC test and expression fold changes were two criteria used to statistically determine differentially expressed proteins between each time set [fold change cutoff = 1, p value cutoff = 0.01, flow direction reversal (FDR) = 0.05]. No normalization, Row Sigma or Total Signal normalization was applied and compared, and differentially expressed proteins satisfied all normalization.

Functional categorization and metabolic pathway analysis

For a protein to be further analyzed in the biological study, the protein needed to be identified in both technical replicates. Functional annotations [Kyoto Encyclopedia of Genes and Genomes (KEGG), Gene Orthology (GO) and Clusters of Orthologous Groups (COGs) databases] of *S. stipitis* were downloaded from the Joint Genome Institute [16]. Proteomes were examined and compared manually with each functional annotation, and in-house Perl scripts were written to perform functional COG counts. The metabolic pathways were visualized using KEGG Mapper [19]. Normalized spectral abundance factors, such as label-free estimation of relative protein abundance, were determined as described in [11].

Results and discussion

Our results represent the first shotgun proteomic study of *S. stipitis* collected at exponential (25-h), late exponential (45.5-h), and early stationary (64-h) stages. Key metabolites, including ethanol, xylose, and xylitol, were measured and monitored throughout *S. stipitis* xylose fermentation (Fig. 1). We observed low xylitol (<0.1 g/L) and low glycerol (<0.2 g/L) throughout the growth cycle. Ethanol 5.86 g/L was achieved at the end of fermentation at 73 h, which resulted in ~30 % theoretical yield. Ethanol formation throughout the growth cycle indicated oxygen limitation, as *S. stipitis* exhibits strictly aerobic growth under fully aerobic conditions. The shotgun approach we used identified and matched peptide mass data to the sequenced *S. stipitis* sequence database (filtered model: 5,839 entries) [16]. Shotgun proteomics enabled observation of the cell proteome and confirmed ~1/6 (17 %) of the predicted open reading frames in the *S. stipitis* genome. Combining all six runs, two technical runs for each time point, we identified 958 proteins throughout fermentation. The complete list of proteins identified for each sample (both technical replicates) is available in the Electronic supplementary material. The false discovery rates of 2D LC–MS/MS runs were from 0.33 % to 4.22 %. It is important to note that the observation of 958 proteins was still an underrepresentation of the *entire S. stipitis* proteome. Through immunodetection, Ghaemmaghami et al. [13] found that ~4,500 proteins (80 %) of *the S. cerevisiae* proteome were expressed during the exponential phase in normal growth conditions.

For a protein to be further analyzed in the biological analysis, only technical replicates from each growth phase were considered. This resulted in identification of 518 proteins at 25-h time set, 526 proteins at 45.5-h time set, and 548 proteins at 64-h time set (Fig. 2). Shotgun proteomics showed highly similar *S. stipitis* proteomes throughout the growth cycle. In general, all three time

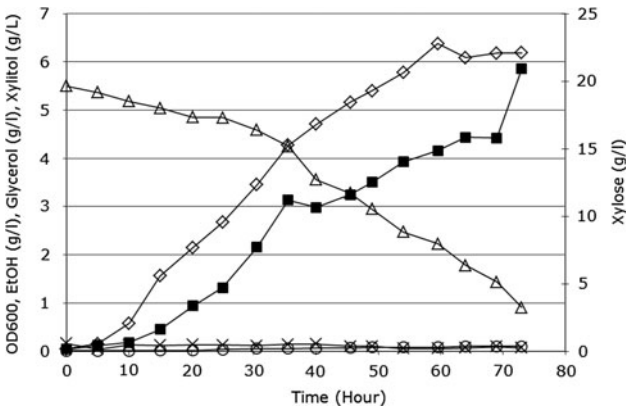

Fig. 1 Ethanol, xylose, xylitol, glycerol, and optical density at 600 nm (OD_{600}) were monitored throughout the growth period of *Scheffersomyces stipitis* xylose fermentation under oxygen limitation. Glycerol and xylitol were detected at a low level, at <0.2 g/L. Fermentation was terminated at 73 h, with final *S. stipitis* OD_{600} at 6.19 and ethanol concentration of 5.86 g/L (~30 % theoretical yield) (*open triangle* xylose, *times symbol* glycerol, *closed box* ethanol, *open diamond* OD_{600}, *open circle* xylitol)

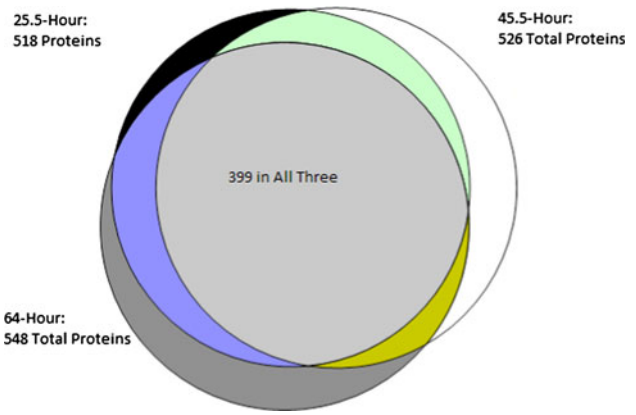

Fig. 2 Numbers of proteins identified (in both technical replicates) at exponential (25-h), late exponential (45.5-h), and early stationary (64-h) phases of *Scheffersomyces stipitis* during xylose fermentation under oxygen limitation. The temporal proteomes exhibited highly similar proteomes throughout growth, with 399 proteins observed between all proteomes, 39 proteins only observed between 25 and 45.5 h, 61 proteins only observed between 45.5 and 64 h, and 18 proteins only observed between 25 and 64 h

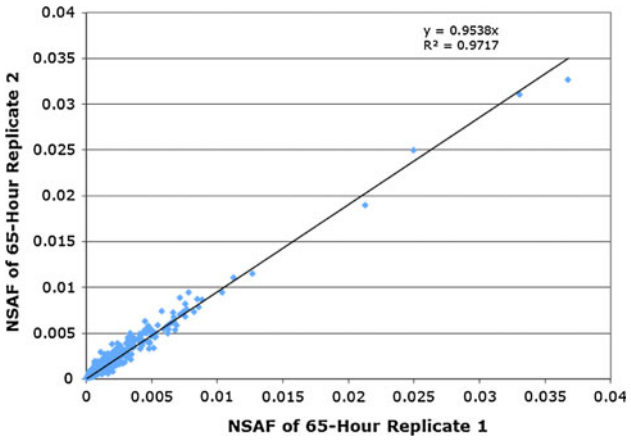

Fig. 3 Comparison of normalized relative abundance factors of two technical runs at early stationary phase (64 h). Each *point* represents a protein identified in both technical replicates 1 and 2. The proteins closer to 0.04 showed higher abundance. R^2 value of 0.97 with slope ~1 showed high reproducibility and consistency between technical duplications

points observed throughout cell growth contained housekeeping processes such as oxidative phosphorylation, glycolysis, nonoxidative branch of the pentose phosphate pathway, gluconeogenesis, biosynthesis of amino acids and aminoacyl-tRNA, protein synthesis and proteolysis, fatty acid metabolism, and cell division. The highly similar proteomes required further statistical analysis to observe how cells progressed throughout the fermentation period.

We calculated normalized spectral abundance factors (NSAFs) to estimate the relative protein abundance of each run. By comparing technical replicates of each data set, we obtained highly reproducible results, with the linear regression line $R^2 = 0.93$ for 25 h, 0.96 for 45.5 h, and 0.97 for 64 h (Fig. 3). The slope of each linear regression close to 1 showed consistency between two technical runs. The most abundant proteins observed throughout xylose fermentation under oxygen limitation came from those of expected processes. Gyceraldehyde-3-phosphate dehydrogenase (Tdh3p), enolase (Eno1p), and phosphoglycerate mutase (Gpm1.1p) involved in glycolysis were highly abundant. The abundance of nicotinamide adenine dinucleotide phosphate, reduced (NADPH)-dependent D-xylose reductase and D-xylulose reductase showed active xylose metabolism shunting xylose into the pentose phosphate pathway and glycolysis [43]. D-xylulokinase (Xks1p) and transketolase (Tkt1p) were also relatively abundant in whole proteomes. The high abundance of mitochondrial porin (Por1p), F_1-F_0-adenosine triphosphatase (ATPase) complex beta subunit (Atp2p) and ubiquinol-cytochrome-c reductase (Cox13p) along with high abundance of alcohol dehydrogenase (Adh1p) showed *P. stipitis* respiration was not repressed at low oxygen. Contrary to the earlier-expression sequence tag data performed by Jeffries et al. [16], Adh1p was actually one of the most abundant proteins observed throughout xylose fermentation, further demonstrating the difference between transcriptomic and proteomic studies. Long-chain fatty acid acyl-coenzyme A (CoA) synthetase (Faa4p) was another highly abundant protein that may have contributed to balancing nicotinamide adenine dinucleotide (NAD+) and nicotinamide adenine dinucleotide phosphate (NADP+)-specific cofactors in xylose fermentation by channeling the reductant into lipid synthesis [16]. Other fatty acid synthase and long chain acyl-CoA synthase (Fas1p and Fas2p) were found throughout the exponential phase but in lower abundance relative to Faa4p. One hypothetical protein (protein model 84089) of unknown function was among the highly abundant protein in log phase. No putative conserved domain was detected on this protein but possibly had as role in eisosome assembly. As mentioned earlier, underrepresentation of the proteome existed, and one limitation was contributed from the bias toward acquisition of more abundant peptide ions, which frequently leads to the identification of low-abundance proteins by one or two peptides [22]. In this experiment, we were not able to identify the essential mitogen-activated protein kinase (MAPK), and only one cyclic adenosine monophosphate (cAMP)-dependent protein kinase regulatory subunit was identified (Protein model 82287), possibly due to their lower abundance.

Proteins identified in each growth phase were classified into COGs functional categories. All three time points showed similar counts in functional attributes, with minor differences. The majority of the protein counts was involved in amino acid transport and metabolism, energy

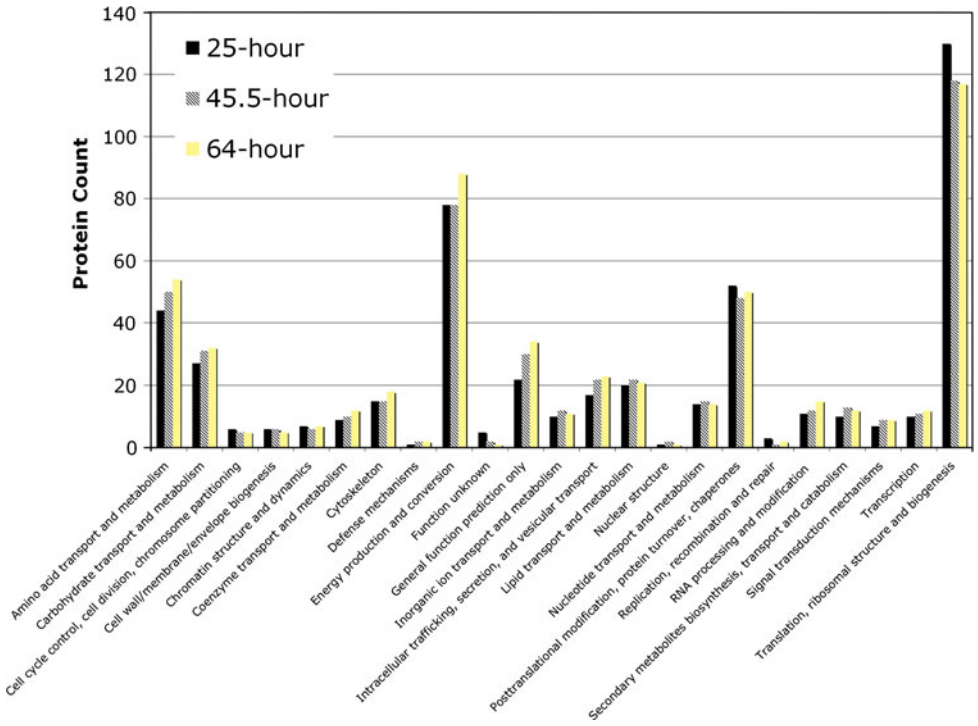

Fig. 4 Comparison of *Scheffersomyces stipitis* proteins identified at 25, 45.5, and 64 h according to Clusters of Orthologous Groups (COGs) for eukaryotic functions. All three proteomes showed similar counts in functional attribute, with minor differences. Protein count in translation-, posttranslational-modification-, and protein-turnover-associated functions were slightly higher at 25 h, whereas protein counts in energy production and conversion function were slightly higher at 64 h

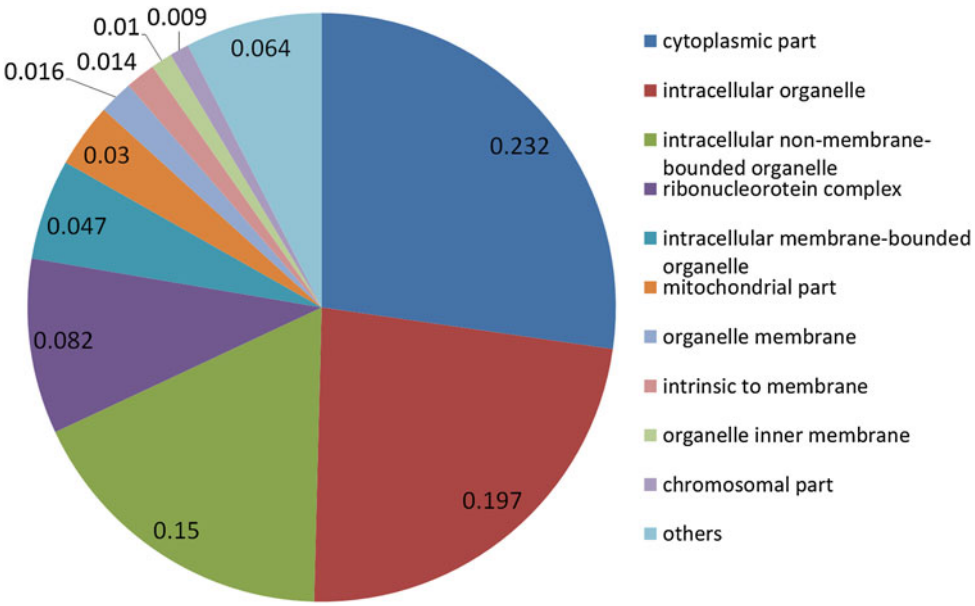

Fig. 5 Gene Ontology (GO) cellular component demonstrated unbiased distribution of *Scheffersomyces stipitis* at 64 h

production and conversion, posttranslational modification, protein turnover, translation, ribosomal structure, and biogenesis (Fig. 4). When comparing the three time points, protein counts in translation, posttranslational modification, and protein turnover functions were slightly higher at 25 h, whereas protein counts in energy production and conversion were slightly higher at 65 h. At the proteome level, the exponential phase exhibited the highest activity in ribosome biogenesis. The overrepresentation of energy production and conversion in the stationary phase may infer adaptation to the different and less efficient carbon or a more complicated carbon metabolism for cell maintenance. The cellular component distribution of identified proteins based on GO showed unbiased distribution of various cellular components, with intracellular parts being the most common; membrane proteins with hydrophobic parts were also obtained (Fig. 5).

We compared KEGG pathway annotations with the temporal proteome and identified the majority of the enzymes involved in citric acid cycle, glycolysis, and the

pentose phosphate pathway. Rate-limiting enzymes, including citrate synthase (Cit1p) in the TCA cycle and glucose-6-phosphate-1-dehydrogenase (Zwf1p) in the pentose phosphate pathway were found throughout the growth period in xylose fermentation. We also obtained all enzymes in the oxoreductive pathway for xylose use, including Xyl1p, Xyl2p, and Xks1p. Ethanol was observed—along with pyruvate decarboxylase (Aro10p), a key enzyme in alcohol fermentation—committed pyruvate of glycolysis to ethanol. Our metabolite data further confirmed the active role of the enzymes involved in glycolysis and xylose use. Throughout the growth phase, we identified a principal enzyme of the glyoxylate cycle: isocitrate lyase (Icl1p), a key enzyme for growth on ethanol and acetate in yeast. We also identified another principal glyoxylate cycle enzyme, malate synthase, at 65 h. In *S. cerevisiae*, *ICL1* expression is tightly regulated, and growth on ethanol requires the glyoxylate pathway for replenishing C4 compounds to the tricarboxylic acid cycle. In *S. cerevisiae*, *ICL1* is induced by growth on ethanol and repressed by growth on glucose [9]. However, our study showed that unlike *S. cerevisiae* metabolism, xylose did not repress Icl1p in *S. stipitis*. As xylose is not a two-carbon compound, the assimilation of xylose into the TCA cycle does not require a glyoxylate cycle. The function of Icl1p in *S. stipitis* xylose fermentation may be to bypasses the catabolic steps of the TCA cycle. This suggests simultaneous biological functions of the glyoxylate cycle and TCA in *S. stipitis* in xylose fermentation under oxygen limitation. The limitations of shotgun proteomics can also been seen in the incomplete pathways identified. Gaps of enzymes existed between metabolites (see Electronic supplementary material for the complete list of enzymes found in the KEGG pathway). Incomplete pathways can be caused by underrepresentation of the whole proteome; however, another key factor is the misannotation of molecular function in enzymes or the protein coding regions, as automated genome/functional annotations contained errors, and the majority of protein sequences in *S. stipitis* have not been experimentally characterized [3, 36].

Another peculiar observation was identification of the alternative oxidase in *S. stipitis* throughout its growth on xylose. We obtained the mitochondrial precursor of salicylhydroxamic acid (SHAM)-sensitive terminal oxidase (Aox1p), which is part of the alternative respiration pathway that consumes oxygen, oxidizes NADH to NAD+, and generates water [37]. Understanding of the SHAM pathway is limited, and contrary to the expression sequence tags data set done earlier by Jeffries et al. [16], we confirmed the expression of Aox1p at the protein level. The SHAM pathway in xylose fermentation could possibly scavenge for oxygen to regenerate reducing equivalents in *S. stipitis* [37]. Observing the SHAM pathway in parallel with the classic respiratory chain may possibly prevent generation of reactive oxygen species (ROS) by limiting ubiquinol auto-oxidation [33].

We obtained uridine diphosphate (UDP) glucose-4-epimerase (Gal10p), both a mutarotase and UDP galactose 4-epimerase [12, 24]. Both are key enzymes in the process of galactose catabolism. In *S. cerevisiae*, galactose genes are highly regulated at the transcription level in response to the specific carbon source. Glucose repressed *GAL* structural genes, and whereas glycerol was poised for low induction, galactose was induced to a high level [23]. However, in our study, we found xylose induction of the Gal10p in *S. stipitis*, suggesting other roles of Gal10p in *S. stipitis*, as galactose was not present in the feedstock medium. Gal10p in *S. stipitis* may infer active interconversion between sugars and possibly to their beta-anomers [24]. We identified the expression of a putative high-affinity xylose sugar transporter Xut1p at 25 and 45.5 h [16]. However, we were not able to identify the low-affinity glucose- and xylose-shared transporters Sut1p, Sut2p, and Sut3p [45]. Adh1p was observed throughout in high abundance, but a secondary zinc-containing alcohol dehydrogenase (Sad2p) was also constitutively expressed throughout. *PsSAD2* shared homology with *ScADH5* in *S. cerevisiae*, and induction under oxygen limitation most likely contributed to the reduction of acetaldehyde to ethanol [16]. Another NADP-dependent alcohol dehydrogenase (Adh4p) was also expressed at mid- and late-log phases, which may be involved in cofactor regeneration under xylose growth. Regulation of various alcohol dehydrogenases in *S. stipitis* largely remained obscure and has been proposed to be regulated by the oxygen level or possibly involved in respiration and regulation of reductants [6]. Xylose may contribute to alcohol dehydrogenase regulation, and further in-depth study is needed to determine the regulatory pathway of alcohol dehydrogenase in *S. stipitis*.

Throughout growth on xylose under oxygen limitation, we obtained the main enzymes involved in glycogen metabolism: glycogen phosphorylase (Gph1p) and glycogen synthase (Gsy1p) [29]. Research in *S. cerevisiae* showed increased Gph1p activity as cells approached the exponential phase, but cells in the early exponential phase under carbon-limited conditions also showed low activity [1]. However, in our study, xylose limitation was introduced. Hence, its expressions may coincide with the roles of glycogen in xylose fermentation in *S. stipitis*. Other stress proteins observed included peroxiredoxin (Prx1p) and thioredoxin reductase (Trr1p), a key regulatory enzyme in the thioredoxin system and that protects cells against both oxidative and reductive stress [34, 41]. Antioxidant activity by thioredoxin seemed essential for growth under oxygen limitation in *P. stipitis* fermentation, as active

mitochondria are the major source of intracellular reactive oxygen species, which could cause upregulation of the antioxidant defense system [25]. We also obtained a nitric oxide oxidoreductase, a flavohemoglobin involved in nitric oxide detoxification and that plays a role in oxidative and nitrosative stress responses [5]. We were not able to obtain xylanase and mannase in our study, but xylose as a sole carbon source induced by a diverse list of *O*-glycosyl hydrolases, including cellulase endo-1,4-beta-glucanase (Bgl5p and Bgl7p), beta-1,3 glucan transferase cell wall glucanase (Scw4p, a glycoside hydrolase, family 17) throughout the growth cycle. Beta-glucosidase family 3 (Bgl2p) was observed at 45.5 and 64 h only, and one chitinase (Ecm33p) was observed, but this is a mucin-like protein, not likely to be involved in degradation of insect or fungal cell wall [16].

Using rich media, we found delta 1-pyrroline-5-carboxylate dehydrogenase (Pro3p), part of the proline biosynthesis, constitutively expressed throughout the growth cycle, as observed in *S. cerevisiae* [2]. The constitutive expression of argininosuccinate synthetase (Arg1p) in *S. stipitis*, which is involved in anabolic arginine biosynthesis and catabolic citrulline, showed that rich medium did not repress *ARG1* [15]. In *S. cerevisiae*, *ARG1* is transcriptionally repressed in the presence of arginine [7]. Glycine dehydrogenase (Gcv2p) expression is induced by glycine and methionine and repressed in rich medium in *S. cerevisiae* [28, 38]. However, we found the constitutive expression of Gcv2p in *S. stipitis* in rich medium. Sulfate adenylyltransferase Met3p in *S. cerevisiae* expression is repressed by the presence of methionine or cysteine [14]. Our proteomics data set suggested either media deficiency or that *S. stipitis* exhibited a different nitrogen pathway. However, metabolic influx studies show that *S. cerevisiae* and *S. stipitis* shared the same amino acid biosynthesis pathway [10].

Although this study focused on qualitative and semi-quantitative analysis, we attempted to identify differentially expressed proteins from the exponential to the stationary phase using the statistical AC test as described earlier. Two proteins are worth mentioning, as they might provide biological insight into the dynamics of fermentation. From the 25 and 45.5 h, Rpl8Ap was downregulated at 30.5-fold. As observed in a previous *S. cerevisiae* study [18], the transcript of ribosomal RNA (rRNA) and ribosomal proteins declined early in the growth cycle, indicating estimation and sensing of available nutrient for potential growth. In the early stationary phase, phosphatidylinositol-specific phospholipase C (PLC) was upregulated at 8.5-fold. In *S. cerevisiae*, phosphatidylinositol-specific PLC generated the signaling molecules diacylglycerol (DAG) and inositol 1,4,5-triphosphate, which have roles in nutrient sensing, phospholipid biosynthesis, growth control, differentiation, and stress-related responses [32].

Conclusion

We successfully employed shotgun proteomics to monitor *S. stipitis* during xylose fermentation under oxygen limitation. This study demonstrates that shotgun proteomics provides an in-depth physiological state, and this technique could be especially useful in less well-studied organisms, such as *S. stipitis*. Limitation existed as under-representation of the entire proteome, but the shotgun proteomics data set provided valuable insights into *S. stipitis* fermentation. In brief, the qualitative study identified the expression of the SHAM pathway, the glyoxylate cycle, and the galactose pathway, suggesting unique expression patterns in *S. stipitis* when compared with the model organism *S. cerevisiae*. Throughout fermentation, qualitative temporal proteomes observed at three time points highly resembled each other, and potential cell dynamics between growth phases was observed, which will need be verified in future studies.

References

1. Becker JU (1982) Mechanisms of regulation of glycogen phosphorylase activity in *Saccharomyces carlsbergensis*. J Gen Microbiol 128:447–454
2. Brandriss MC, Falvey DA (1992) Proline biosynthesis in *Saccharomyces cerevisiae*: analysis of the PRO3 gene, which encodes delta 1-pyrroline-5-carboxylate reductase. J Bacteriol 174:3782–3788
3. Brent MR (2008) Steady progress and recent breakthroughs in the accuracy of automated genome annotation. Nat Rev Genet 9:62–73
4. Carvalho PC, Fischer JSG, Chen EI, Yates JR, Barbosa VC (2008) PatternLab for proteomics: a tool for differential shotgun proteomics. BMC Bioinform 9:316–329
5. Cassanova N, O'Brien KM, Stahl BT, McClure T, Poyton RO (2005) Yeast flavohemoglobin, a nitric oxide oxidoreductase, is located in both the cytosol and the mitochondrial matrix. J Biol Chem 280:7645–7653
6. Cho JY, Jeffries TW (1999) Transcriptional control of ADH genes in the xylose-fermenting yeast *Pichia stipitis*. Appl Environ Microbiol 65:2363–2368
7. Crabeel M, Lavalle R, Glansdorff N (1990) Arginine-specific repression in *Saccharomyces cerevisiae*: kinetic data on ARG1 and ARG3 mRNA transcription and stability support a transcriptional control mechanism. Mol Cell Biol 10:1226–1233
8. Eng JK, McCormack AL, Yates JR (1994) An approach to correlate tandem mass spectra data of peptides with amino acid sequences in a protein database. J Am Soc Mass Spectrom 5:976–989
9. Fernandez E, Moreno F, Rodicio R (1992) The ICL1 gene from *Saccharomyces cerevisiae*. Eur J Biochem 204:983–990
10. Fiaux J, Cakar ZP, Sonderegger M, Wuthrich K, Szyperski T, Sauer U (2003) Metabolic-flux profiling of the yeasts *Saccharomyces cerevisiae* and *Pichia stipitis*. Eukaryot Cell 2:170–180

11. Florens L, Carozza MJ, Swanson SK, Fournier M, Coleman MK, Workman JL, Washburn MP (2006) Analyzing chromatin remodeling complexes using shotgun proteomics and normalized spectral abundance factors. Methods 40:303–311
12. Fukasawa T, Obonai K, Segawa T, Nogi Y (1980) The enzymes of the galactose cluster in *Saccharomyces cerevisiae*. II. Purification and characterization of uridine diphosphoglucose 4-epimerase. J Biol Chem 255:2705–2707
13. Ghaemmaghami S, Huh WK, Bower K, Howson RW, Belle A, Dephoure N, O'Shea EK, Weissman JS (2003) Global analysis of protein expression in yeast. Nature 425:737–741
14. Gierest H, Thao NN, Surdin-Kerjan Y (1985) Transcriptional regulation of the MET3 gene of *Saccharomyces cerevisiae*. Gene 34:269–281
15. Jauniaux JC, Urrestarazu LA, Wiame JM (1978) Arginine metabolism in *Saccharomyces cerevisiae*: subcellular localization of the enzymes. J Bacteriol 133:1096–1107
16. Jeffries TW, Grigoriev IV, Grimwood J, Laplaza JM, Aerts A, Salamov A, Schmutz J, Lindquist E, Dehal P, Shapiro H (2007) Genome sequence of the lignocellulose-bioconverting and xylose-fermenting yeast *Pichia stipitis*. Nat Biotechnol 25:319–326
17. Jeffries TW, Van Vleet JRH (2009) Pichia stipitis genomics, transcriptomics, and gene clusters. FEMS Yeast Res 9:793–807
18. Ju Q, Warner JR (1994) Ribosome synthesis during the growth cycle of *Saccharomyces cerevisiae*. Yeast 10:151–157
19. Kanehisa M, Goto S (1999) KEGG: Kyoto encyclopedia of genes and genomes. Nucleic Acids Res 27:29–34
20. Lin FM, Qiao B, Yuan YJ (2009) Comparative proteomic analysis of tolerance and adaptation of ethanologenic *Saccharomyces cerevisiae* to furfural, a lignocellulosic inhibitory compound. Appl Environ Microbiol 75:3765–3776
21. Link AJ, Eng J, Schieltz DM, Carmack E, Mize GJ, Morris DR, Garvik BM, Yates Iii JR (1999) Direct analysis of protein complexes using mass spectrometry. Nat Biotechnol 17:676–682
22. Liu H, Sadygov RG, Yates Iii JR (2004) A model for random sampling and estimation of relative protein abundance in shotgun proteomics. Anal Chem 76:4193–4201
23. Lohr D, Venkov P, Zlatanova J (1995) Transcriptional regulation in the yeast GAL gene family: a complex genetic network. FASEB J 9:777–787
24. Majumdar S, Ghatak J, Mukherji S, Bhattacharjee H, Bhaduri A (2004) UDPgalactose 4 epimerase from *Saccharomyces cerevisiae*. Eur J Biochem 271:753–759
25. Maris AF, Assumpcao ALK, Bonatto D, Brendel M, Henriques JAP (2001) Diauxic shift-induced stress resistance against hydroperoxides in *Saccharomyces cerevisiae* is not an adaptive stress response and does not depend on functional mitochondria. Curr Genet 39:137–149
26. McDonald WH, Ohi R, Miyamoto DT, Mitchison TJ, Yates JR (2002) Comparison of three directly coupled HPLC MS/MS strategies for identification of proteins from complex mixtures: single-dimension LC-MS/MS, 2-phase MudPIT, and 3-phase MudPIT. Int J Mass 219:245–251
27. Milburn M (2009) Using metabolic profiling technology to advance cell culture development. Biopharm international JUN, pp 28–34
28. Nagarajan L, Storms RK (1997) Molecular characterization of GCV3, the *Saccharomyces cerevisiae* gene coding for the glycine cleavage system hydrogen carrier protein. J Biol Chem 272:4444–4450
29. Ni HT, LaPorte DC (1995) Response of a yeast glycogen synthase gene to stress. Mol Biol 16:1197–1205
30. Peng J, Elias JE, Thoreen CC, Licklider LJ, Gygi SP (2003) Evaluation of multidimensional chromatography coupled with tandem mass spectrometry (LC/LC–MS/MS) for large-scale protein analysis: the yeast proteome. J Proteome Res 2:43–50
31. Ram RJ, VerBerkmoes NC, Thelen MP, Tyson GW, Baker BJ, Blake RC, Shah M, Hettich RL, Banfield JF (2005) Community proteomics of a natural microbial biofilm. Science 308:1915–1920
32. Rebecchi MJ, Pentyala SN (2000) Structure, function, and control of phosphoinositide-specific phospholipase C. Physiol Rev 80:1291–1335
33. Rosenfeld E, Beauvoit B, Rigoulet M, Salmon JM (2002) Non-respiratory oxygen consumption pathways in anaerobically-grown *Saccharomyces cerevisiae*: evidence and partial characterization. Yeast 19:1299–1321
34. Ross SJ, Findlay VJ, Malakasi P, Morgan BA (2000) Thioredoxin peroxidase is required for the transcriptional response to oxidative stress in budding yeast. MBoC 11:2631–2642
35. Ryabova O, Vrsansk M, Kaneko S, van Zyl WH, Biely P (2009) A novel family of hemicellulolytic [alpha]-glucuronidase. FEBS Lett 583:1457–1462
36. Schnoes AM, Brown SD, Dodevski I, Babbitt PC (2009) Annotation error in public databases: misannotation of molecular function in enzyme superfamilies. PLoS Comput Biol 5:e100 0605
37. Shi NQ, Cruz J, Sherman F, Jeffries TW (2002) SHAM sensitive alternative respiration in the xylose metabolizing yeast *Pichia stipitis*. Yeast 19:1203–1220
38. Sinclair DA, Hong SP, Dawes IW (1996) Specific induction by glycine of the gene for the P subunit of glycine decarboxylase from *Saccharomyces cerevisiae*. Mol Microbiol 19:611–623
39. Sivagnanam K, Raghavan V, Shah M, Hettich R, Verberkmoes N, Lefsrud M (2011) Comparative shotgun proteomic analysis of *Clostridium acetobutylicum* from butanol fermentation using glucose and xylose. Proteome Sci 9:66
40. Thompson MR, Chourey K, Froelich JM, Erickson BK, VerBerkmoes NC, Hettich RL (2008) Experimental approach for deep proteome measurements from small-scale microbial biomass samples. Anal Chem 80:9517–9525
41. Trotter EW, Grant CM (2002) Thioredoxins are required for protection against a reductive stress in the yeast *Saccharomyces cerevisiae*. Mol Microbiol 46:869–878
42. Verberkmoes NC, Russell AL, Shah M, Godzik A, Rosenquist M, Halfvarson J, Lefsrud MG, Apajalahti J, Tysk C, Hettich RL (2008) Shotgun metaproteomics of the human distal gut microbiota. ISME J 3:179–189
43. Verduyn C, Van Kleef R, Frank J, Schreuder H, Van Dijken JP, Scheffers WA (1985) Properties of the NAD (P) H-dependent xylose reductase from the xylose-fermenting yeast *Pichia stipitis*. Biochem J 226:669–677
44. Washburn MP, Wolters D, Yates JR III (2001) Large-scale analysis of the yeast proteome by multidimensional protein identification technology. Nat Biotechnol 19:242–247
45. Weierstall T, Hollenberg CP, Boles E (1999) Cloning and characterization of three genes (SUT1-3) encoding glucose transporters of the yeast *Pichia stipitis*. Mol Microbiol 31:871–883
46. Wilmes P, Andersson AF, Lefsrud MG, Wexler M, Shah M, Zhang B, Hettich RL, Bond PL, VerBerkmoes NC, Banfield JF (2008) Community proteogenomics highlights microbial strain-variant protein expression within activated sludge performing enhanced biological phosphorus removal. ISME J 2:853–864
47. Wolters DA, Washburn MP, Yates JR III (2001) An automated multidimensional protein identification technology for shotgun proteomics. Anal Chem 73:5683–5690